

REVIEW

[View Article Online](#)
[View Journal](#) | [View Issue](#)Cite this: *J. Mater. Chem. B*, 2025,
13, 11148Recent advances and biomedical applications
of conductive hydrogels for wound repairYawen Wang,^{ac} Tong Wu,^{id} *^c Xiumei Mo^{id} *^b and Yuanfei Wang^{id} *^d

The skin, serving as the body's primary line of defense against external elements, is easily damaged, forming acute or chronic wounds. Consequently, wound care has generated significant market demand and attracted considerable interest. Conductive hydrogels, cutting-edge materials that effectively merge the extracellular matrix mimicking properties of hydrogels with the electrochemical properties of conductive materials, have garnered substantial attention in tissue engineering. In addition to the unique mechanical adjustability and bioactive substance transport capabilities of hydrogels, conductive hydrogels provide endogenous electric fields and injury currents to the wound area through electrical stimulation, enhancing cell migration and the development of epithelial layers. Therefore, they possess significant potential for practical application in skin wound repair. This article reviews the applications and recent advancements of conductive hydrogels in wound healing over the past five years, including the types and characteristics of conductive hydrogels and their use in various kinds of wounds, and evaluates the limitations and prospects of conductive hydrogels, offering references and new insights for their future clinical applications.

Received 11th May 2025,
Accepted 8th August 2025

DOI: 10.1039/d5tb01130b

rsc.li/materials-b

Introduction

The skin is the largest organ in the human body and is crucial in protecting us from external damage.¹ Acting as the main physical barrier between our body and the external environment, the skin performs essential functions like regulating body temperature, sensing stimuli, and maintaining homeostasis.² However, being the most exposed layer, the skin is vulnerable to injury and damage. Persistent structural damage leads to various wound levels. Healing these wounds necessitates a series of continuous and coordinated biochemical processes.³ Skin wounds are generally divided into acute wounds and chronic wounds according to the duration of the wound healing.⁴ After undergoing four fundamental stages – hemostasis, inflammation, proliferation, and remodeling (Fig. 1),⁵ acute wounds, such as mechanical injuries, chemical injuries, and surgical wounds, usually take 8 to 12 weeks to recover fully.⁶ Chronic wounds such as burns, infections, and those related to diabetes are more difficult to heal and require a

longer time for recovery. Adverse reactions from injuries can lead to infections and the formation of bacterial biofilms.^{7,8} In addition, excessive reactive oxygen species (ROS) and impaired vascular function in diabetic wound healing often halt recovery during inflammation, hindering proper healing.^{9–11} Serious chronic wounds often lead to amputation, sepsis, or even death if untreated promptly.¹² Thus, adequate wound care is vital to avoid infections and foster healing.

As an essential method of wound management, dressings can prevent external wound contamination. Traditional dressings include gauze, cotton, and bandages.¹³ These wound dressings mainly protect against contaminants rather than healing wounds, thus offering limited benefits for chronic wounds.⁴ Additionally, traditional dressings are usually dry and non-degradable, requiring regular changes. However, since they cannot provide a moist environment, these dressings tend to adhere to the wound as the exudate solidifies, causing secondary injury.⁶ In reference to the problem mentioned above, various innovative biological materials have been created for wound healing.^{14–17} Chitosan is a key research material with its antibacterial and efficient hemostatic functions. Synthetic polymers like polylactic acid (PLA) and polycaprolactone (PCL), known for their strength and controlled breakdown, are used in skin tissue engineering. Among these, hydrogels, highly hydrophilic macromolecular 3D networks, are expected to significantly benefit the biomedical field after undergoing physical or chemical crosslinking to form biomaterials with high water absorption and swelling properties.^{18,19} Studies have

^a School of Rehabilitation Sciences and Engineering, University of Health and Rehabilitation Sciences, Qingdao 266113, China^b Institute of Biomaterials and Biomedicine, School of Food and Pharmacy, Shanghai Zhongqiao Vocational and Technical University, Shanghai 201514, China. E-mail: xmm@dhu.edu.cn^c Medical Research Center, The Affiliated Hospital of Qingdao University, Qingdao University, Qingdao 266000, China. E-mail: twu@qdu.edu.cn^d Qingdao Stomatological Hospital Affiliated to Qingdao University, Qingdao 266001, China. E-mail: zhizunbao19@163.com

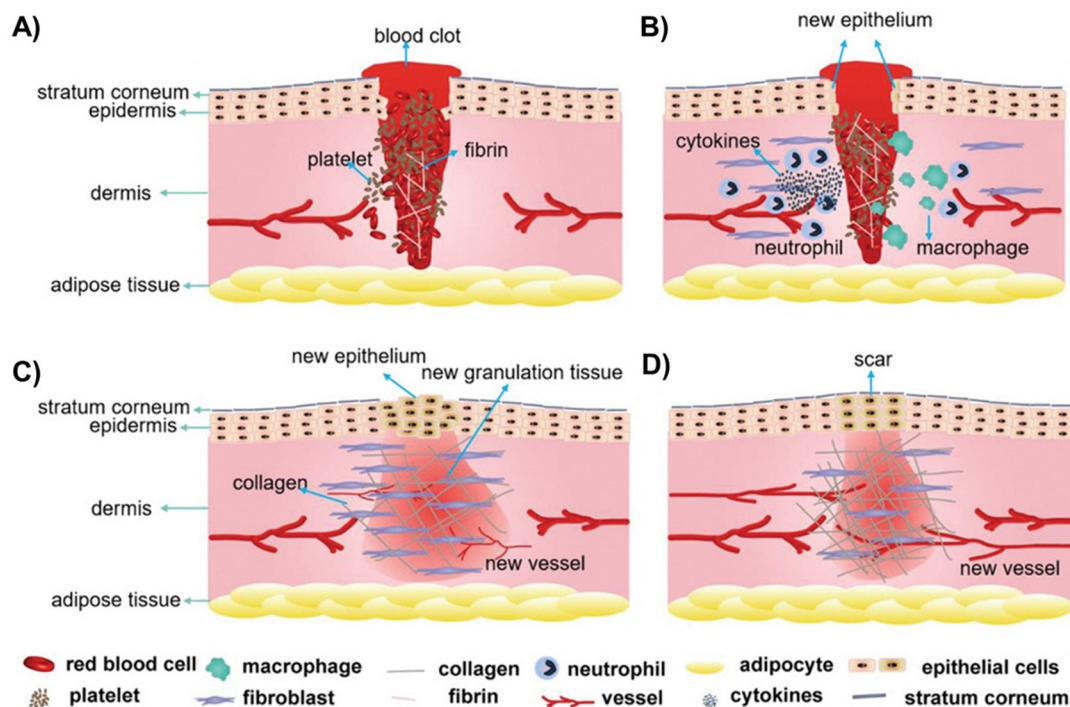


Fig. 1 The processes of wound healing: (A) hemostasis, (B) inflammation, (C) proliferation and (D) remodeling.⁵ Reproduced from ref. 5 with the permission of Wiley-VCH GmbH, copyright 2021.

demonstrated that skin cells regenerate more efficiently in a moderate humidity environment.²⁰ Exogenous electrical stimulation (ES), by emulating the endogenous currents at the wound site, contributes actively to the process of wound healing.^{21–23} Hydrogels mimic the extracellular matrix's (ECM) 3D environment, enhancing cell adhesion, growth, and differentiation to expedite healing. As wound dressings, they absorb excess fluids, starve bacteria, and promote breathability.²⁴ Therefore, applying hydrogels in wound healing is worthy of long-term, in-depth research.

Skin tissue possesses electro-sensitivity,²⁵ the uneven distribution of ion channels within the epidermal cells enables the intact epidermis to maintain an electrical potential difference, while the movement of ions ensures a stable trans-epidermal potential (TEP).²⁶ Upon skin injury, the disruption of the TEP leads to the immediate generation of an endogenous electric field (EF) and damage current, which assist in cell migration and the re-epidermalization process. By emulating the endogenous currents at the wound site, exogenous ES actively contributes to the wound healing process.^{22,23} However, traditional ES requires electrodes close to the wound to deliver currents, which is not ideal for wide-area injuries. To address this, conductive hydrogels have been developed by combining hydrogels and conductive properties, providing biomimetic and electrochemical benefits for wound healing.^{27,28}

Considering the previously mentioned issues, this paper provides an extensive review of the uses of conductive hydrogels in wound healing applications over the past five years, as illustrated in the overall schematic diagram of conductive hydrogels for wound repair shown in Fig. 2. To begin with, we categorize the diverse types of conductive hydrogels and highlight

several prototypical examples. Thereafter, we explore the multifaceted properties exhibited by conductive hydrogels. In subsequent sections, we investigate the applications of conductive hydrogels in various wound repair scenarios, covering acute and chronic wounds. Finally, we discuss the biosafety of conductive hydrogels and the prospects of conductive hydrogels in traumatic repair, providing a scientifically robust perspective that informs the potential applications of these materials in wound care.

Classification of conductive hydrogels

Conductive hydrogels based on conductive polymers

Conductive polymers are macromolecules with a conjugated framework, endowing them with distinctive electrical and optical qualities. Their conductivity stems from the efficient delocalization of π -electrons along the polymer's backbone, enabling charge flow and establishing their conductive nature.²⁹ Various conductive polymers, such as polythiophene (PTh), polypyrrole (PPy), and polyaniline (PANI), exhibit a tunable range of electrical conductivity upon doping and surface functionalization. Due to their inherently hydrophobic nature stemming from the aromatic rings in their frameworks, conductive polymers are integrated into hydrogel matrices through methods such as grafting and doping to create conductive hydrogels with uniform dispersion and stability properties,³⁰ thereby expanding their biomedical applications.^{29,31}

Poly(3,4-ethylene dioxythiophene) (PEDOT), one of the most widely used hydrophobic PTh, can be easily dispersed in aqueous buffer solutions when coated with a hydrophilic poly(styrene sulfonate) (PSS) shell to form PEDOT:PSS

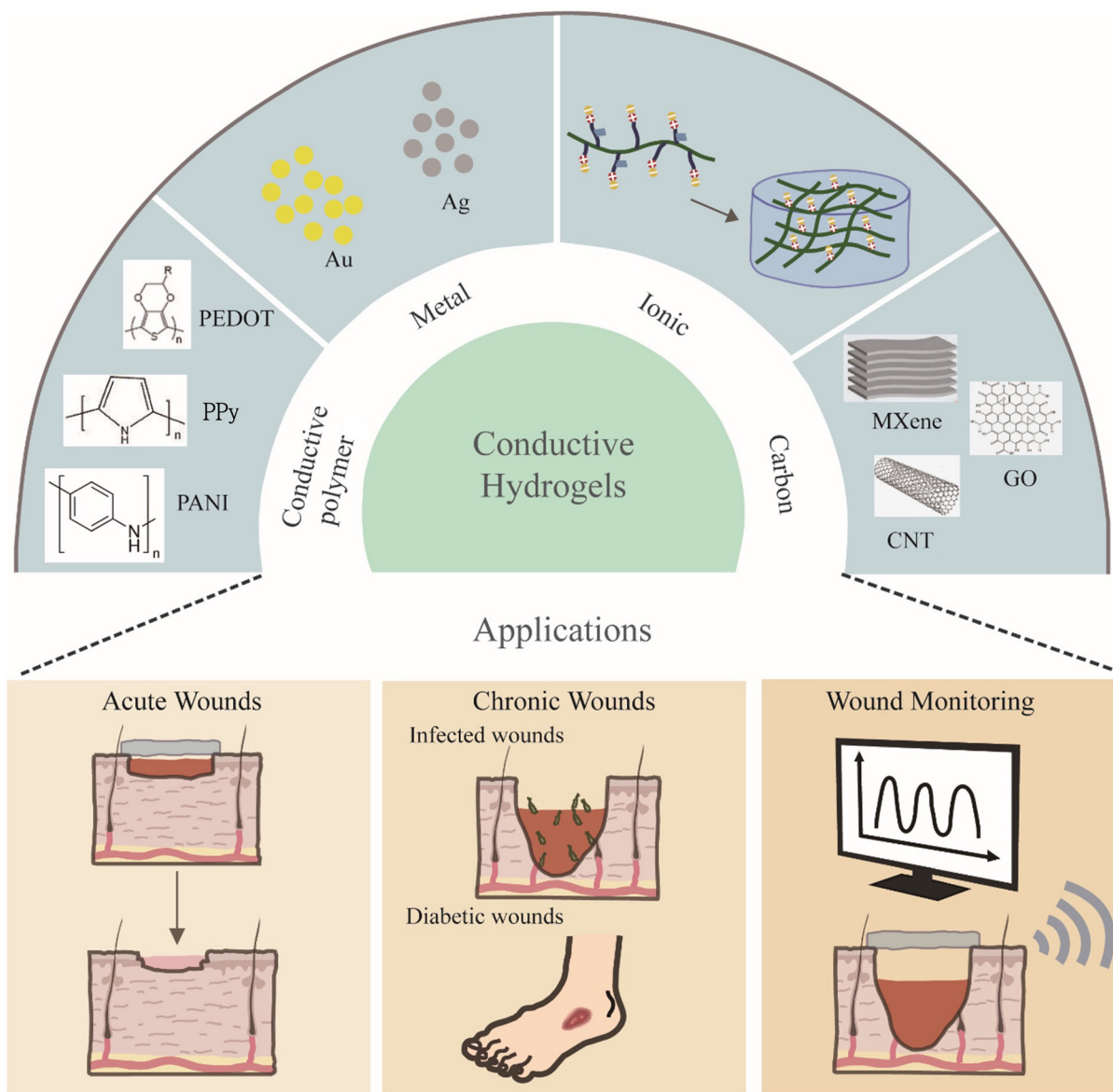


Fig. 2 The overall schematic diagram of conductive hydrogels for wound repair.

nanoparticles (NPs), exhibiting high conductivity, high transparency, and high flexibility.³² A study demonstrated the synthesis of pure PEDOT:PSS hydrogels by adding dimethyl sulfoxide (DMSO) to the polymer solution. The hydrogels' electrical, mechanical, and swelling characteristics were systematically modulated through DMSO concentration and drying/annealing procedures.³³ Recently, as shown in Fig. 3A, a highly 3D-printable PEDOT:PSS-based ink has been successfully fabricated for tissue engineering. Enhanced with freeze-dried PEDOT:PSS and carbon nanotubes, the ink yields a hydrogel post-printing with a remarkable conductivity of 2000 S m^{-1} . It boasts superior elasticity, aqueous stability, durability, electromagnetic shielding, and sensing abilities, positioning it as a promising candidate for tissue engineering technologies.³⁴ Notably, the carbon nanotubes in the ink are also a conductive material widely utilized in fabricating conductive hydrogels,

which will be described in detail in the following text. A novel study resulted in the formulation of a conductive hydrogel by incorporating metal halides into PEDOT:PSS, which can significantly enhance its conductivity while allowing for adjustable shapes and stretchability. The metal halides' cations, acting as Lewis acids, form a complex with the PSS anions, promoting phase separation.³⁵ Beyond the use of PSS involved an anionic polysaccharide template dispersion strategy to develop a specialized tissue engineering dispersion system consisting of PEDOT:(dextran sulfate/carboxymethyl chitosan) (PEDOT:(DSS/CMCS)). This system, formed through a mild Schiff base reaction, yielded injectable conductive hydrogels. PEDOT:(DSS/CMCS) showed enhanced tissue compatibility and effectively delivered adipose-derived stem cells, promoting angiogenesis.³⁶ In brief, hydrogels based on PEDOT, distinguished by their remarkable conductive and flexible characteristics, have become prevalent

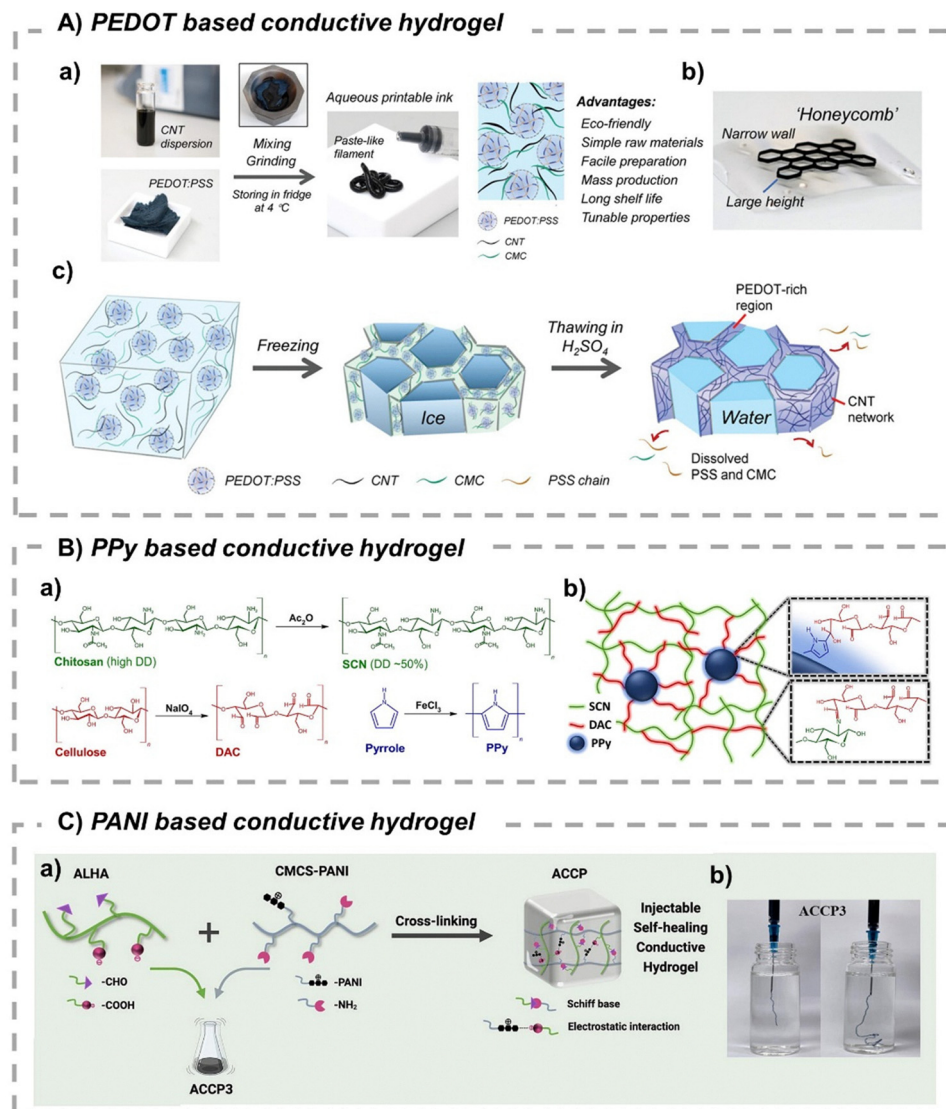


Fig. 3 Conductive hydrogels based on conductive polymers. (A) PEDOT-based conductive hydrogels. (a) Preparation process of the composite inks for 3D printing. (b) Photographs of a printed architecture. (c) Schematic illustrating the gelation process of the printed device during the post-printing process. Reproduced from ref. 34 with the permission of Wiley-VCH GmbH, copyright 2023. (B) PPy-based conductive hydrogels. (a) Scheme of synthesis of SCN, DAC, and PPy. (b) Representation of SCN/DAC_PPy hydrogel with details of bonding between DAC and PPy (top) and DAC and SCN (bottom). Reproduced from ref. 39 with the permission of Elsevier, copyright 2023. (C) PANI-based conductive hydrogels. (a) Schematic diagram of the preparation of an injectable conductive hydrogel. (b) Injectable property of the ACCP3 hydrogel. Reproduced from ref. 45 with the permission of Elsevier, copyright 2023.

in tissue engineering endeavors and symbolize a bountiful potential for advancement.

PPy is a polymer with a high degree of π -conjugation in its polymer chain, which imparts inherent electrical conductivity. It exhibits controllable electrical conductivity, thermal stability, and environmental resilience.^{37,38} In a research endeavor, a conductive hydrogel featuring covalently bound PPy NPs was developed through the crosslinking of chitosan with divalent alcohol cellulose (DAC) and the covalent anchoring of PPy colloidal particles. This hydrogel captures ROS, has tissue-like conductivity, and adheres to the skin, offering potential applications in skin wound therapy (Fig. 3B).³⁹ In another study, a novel and easily synthesizable agarose/gelatin/PPy hydrogel (Aga/Gel/PPy, AGP3) was developed by modulating the

concentrations of Aga and PPy. It boasts enhanced conductivity via an *in situ* PPy network and improved thermal stability at physiologic temperatures. Its physical cross-linking enables injection, and the hydrogel's modulus is easily controllable through Aga dosage.⁴⁰ Recent research utilizes the microemulsion method to synthesize PPy NPs, which are then incorporated into a Gel-hyaluronic acid (HA) composite hydrogel. The resulting HA:PPy-NPs hydrogel, designed for tissue engineering, exhibits exceptional mechanical properties and significant cytocompatibility, improving cell adhesion and proliferation.⁴¹ Moreover, a gel-based hydrogel containing PPy was developed, using tannic acid (TA) as a crosslinker to enable dynamic non-covalent bonding. The role of TA in doping PPy was crucial for determining the electrical conductivity of the hydrogel.⁴²

PANI, a commonly utilized conductive polymer known for its high electrical conductivity,^{43,44} was recently modified to be grafted onto CMCS, synthesizing a novel water-soluble conductive material. Incorporating this material into a dynamic gel network formed through a Schiff base reaction between aldehyde-functionalized HA (ALHA) and CMCS creates a dual-crosslinked hydrogel. This hydrogel possesses injectability, self-healing properties, and conductivity, while also demonstrating good biocompatibility, elastic modulus, and electrical conductivity (Fig. 3C).⁴⁵ Moreover, employing a “doping followed by gelling” approach, a PANI/poly(acrylic acid) (PAA) hydrogel was synthesized with a unique chain entangled network. The strong electrostatic interactions between PAA and PANI chains act as dynamic crosslinks, endowing the hydrogel with electrical conductivity and exceptional properties, including super-stretchability, high tensile strength, and rapid self-healing capabilities.⁴⁶

Although conductive hydrogels based on conductive polymers have reached a certain level of development, issues regarding the uneven dispersion of conductive polymers persist, and most polymer monomers are toxic. Consequently, polymer residues may remain in the body in clinical applications, posing potential risks that are difficult to metabolize. Therefore, exploring the biodegradability of these materials is essential, such as by combining conductive polymers with degradable polymers to enhance the degradation ability and biocompatibility of conductive hydrogels.

Conductive hydrogels based on metal nanomaterials

Metals are known for their high electrical conductivity, ease of manipulation, and properties such as corrosion resistance, oxidation resistance, and high specific surface.⁴⁷ Valence electrons in metals, combined with their high crystallinity, facilitate conductivity. Moreover, most metal NPs exhibit biocompatibility, rendering them inherently antibacterial, antiviral, and anti-inflammatory. Consequently, conductive hydrogels fabricated with metal nanomaterials have garnered significant interest in tissue repair in recent years.^{48–50}

Gold is a prevalent metal in biomedical applications among various metals, with gold NPs (Au-NPs) and nanorods being utilized in fabricating carbon nanotubes. The integration of Au-NPs with a dual aldehyde polyurethane (DAPU) nanocrosslinker, followed by the addition of O-CMC (Fig. 4A), results in the formation of a conductive hydrogel with self-healing and anti-inflammatory capabilities. This hydrogel can exert anti-inflammatory and protective effects on inflamed neural stem cells.⁵¹ Empirically distinguished for their conductivity and stability, Au-NPs offer a substantial prospect for advancements in cardiac tissue engineering,^{52–54} notably through the fusion with conductive hydrogels. A salient example unfolds with the formation of an *in situ* hydrogel through the merger of the hyperbranched polymer polyethylene glycol diacrylate/4-vinylbenzyl boric acid (PEGDA-PBA) and thiolated HA (HA-SH). Such a hydrogel attains a heightened capability for medicinal targeting and delivery upon being loaded with astragaloside (AST) NPs. The additive incorporation of gold nanorods into this matrix translates to endowing the scaffold with conductive

capabilities, thereby proposing a cutting-edge therapeutic intervention for mitigating the impacts of myocardial infarction.⁵⁵ Furthermore, Au-NPs can be synthesized *in situ* in the presence of lysozyme nanofibrils (LNFs). The resulting hybrid AuNPs@LNFs are then dispersed within Gel-HA hydrogels. The obtained hydrogels display enhanced rheological behavior, mechanical resilience, antioxidant activity, and electrical conductivity, which benefit myocardial regeneration applications.⁵⁶

Apart from gold, silver is the most extensively employed metal in biological materials among all common metals. Silver-based biomedical materials, in addition to their conductive properties, possess robust antibacterial abilities and are widely used to treat burns and infected wounds. Polydopamine-functionalized silver (PDA@Ag) NPs, in combination with 3-aminophenyl boronic acid, PPy, and polyvinyl alcohol (PVA), can self-assemble into a multifunctional conductive hydrogel *via* supramolecular interactions (Fig. 4B). This hydrogel exhibits excellent electrical and mechanical properties, as well as broad-spectrum antibacterial activity, and has a significant therapeutic effect on diabetic foot wounds.⁵⁷ In an innovative research effort, motivated by the adhesive properties of mussels, TA was reacted with ultra-small Ag NPs through an *in situ* reduction process to form tannic acid-chelated silver (TA-Ag) nanoenzymes. These nanoenzymes induced the autocrosslinking of the hydrogel without requiring external agents. The uniform distribution of the nanoenzymes, which possess phenolic groups, within the hydrogel network contributed to the hydrogel's improved mechanical and electrical properties.⁵⁸ Another scientifically rigorous experiment demonstrated that lignin NPs can catalyze the *in situ* reduction of silver to form silver-lignin NPs. In conjunction with Fe³⁺, ammonium persulfate (APS), and acrylic acid (AA), this composite material enables the ultra-fast polymerization of PAA at room temperature within just a few minutes. As a result, the former hydrogel exhibited exceptional electrical conductivity, UV resistance, and high antibacterial activity.⁵⁹ To enhance the biosafety of conductive hydrogels, combined with the biocompatible and highly antibacterial Ag NPs, a novel approach utilizing natural polymers without chemical reducing agents was employed. This method involved the *in situ* photoreduction of silver ions and the semi-dissolution acidification sol-gel transition, which resulted in the creation of a multifunctional chitosan/CMCTS/Ag NPs (CTS/CMCTS/Ag NPs) conductive hydrogel, which exhibited enhanced mechanical strength, self-healing ability, and biocompatibility.⁶⁰

With their outstanding electrical conductivity and ease of preparation, metal nanomaterials have emerged as a preferred choice for fabricating conductive hydrogels. Conductive hydrogels based on metal nanomaterials have also achieved extensive development. However, most metals are toxic, which limits the application of conductive hydrogels based on metal nanomaterials in wound repair.

Ionic conductive hydrogels

Unlike the traditional approach of adding conductive particles to hydrogels for conductivity, injecting a high concentration of free ions into the hydrogel's polymer network can simultaneously

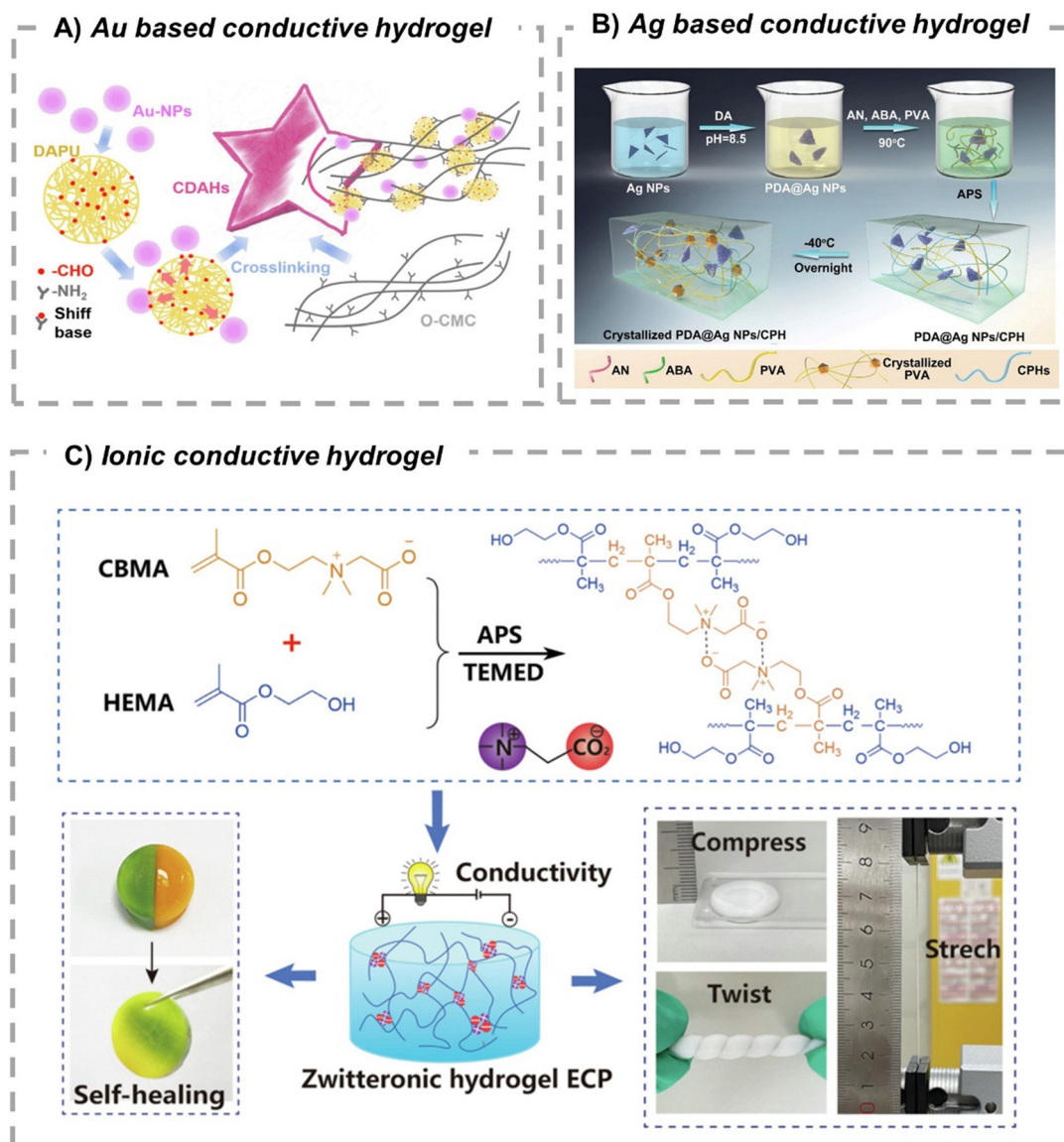


Fig. 4 Conductive hydrogels based on metal nanomaterials. (A) Au-based conductive hydrogels. Reproduced from ref. 51 with the permission of Elsevier, copyright 2022. (B) Ag-based conductive hydrogels. Reproduced from ref. 57 with the permission of Wiley-VCH GmbH, copyright 2019. (C) Ionic conductive hydrogels: Schematic illustration of the zwitterionic hydrogel. Reproduced from ref. 64 with the permission of Wiley-VCH GmbH, copyright 2022.

result in a hydrogel with excellent ionic conductivity, rapid gelation, injectability, and high elasticity.⁶¹ The homogeneous arrangement of conductive ions within the hydrogel matrix addresses the mechanical and electrical drawbacks of the aggregation observed in traditional electronically conductive hydrogels. This configuration enables a more accurate simulation of ion transport found in tissue cells, thereby providing a continuous conductive microenvironment that supports the healing of skin wounds, representing a novel approach to applying conductive hydrogels in tissue restoration.⁶²

For instance, integrating TA and human-like collagen (HLC) into a PVA and borax crosslinking network creates an adaptive conductive hydrogel. Borax is both a crosslinker and an ionic conductor, providing conductivity, adaptability, and self-healing

properties to the hydrogel through dynamic crosslinking mediated by borate bonds. The introduction of HLC and TA alters the hydrogel's crosslinking density and pH, providing the hydrogel with functions such as hemostasis, antimicrobial activity, anti-inflammatory properties, cell proliferation, and collagen deposition. Furthermore, this hydrogel enables the transmission of endogenous and exogenous electrical currents, facilitating intercellular signaling and the transfer of electrical stimuli, which in turn promote cell migration and angiogenesis.²²

Another innovative conductive hydrogel incorporated PDA NPs, glucose oxidase (GOx), and catalase (CAT) into a PDA/acrylamide (AM) hydrogel matrix. The presence of GOx enhanced the hydrogel's adhesiveness, glucose-lowering potency, and superior conductivity, thereby speeding up the

wound healing process.⁶³ Furthermore, conductive amphiphilic ionic hydrogels were prepared using the co-polymerization of diblock ionic monomers, such as methyl acrylate carbobetaine (CBMA), and biocompatible monomers, such as methyl acrylate hydroxyethyl ether (HEMA). The hydrogels demonstrated outstanding ionic conductivity, commendable mechanical properties, including compression and tension, self-healing abilities, and mechanosensory functions, rendering them applicable for the repair of myocardial tissue injuries (Fig. 4C).⁶⁴

Currently, the conductivity of ionic hydrogels primarily depends on the free movement of anions and cations. However, the internal structure of hydrogels often restricts ion movement, affecting their conductive properties. Moreover, toxicity and ion leakage are significant issues for ionic hydrogels, which limit their development in wound healing and require particular attention.

Conductive hydrogels utilizing carbon-based nanomaterials

With their impressive environmental stability, high electrical conductivity, and large specific surface area, carbon-based materials have gained extensive applications in biomolecule functionalization and the modulation of cellular responses to injury repair.^{65,66} This category includes materials such as carbon nanotubes (CNTs), graphene, activated carbon, carbon fibers, carbon dots, and porous carbon nanotubes, with CNTs and graphene serving as the most illustrative examples in the creation of conductive hydrogels.^{23,67} As shown in Fig. 5A, by uniformly coating a covalent organic framework (COF) on oxidized carbon nanotubes (OCNTs) and coordinating it with Fe^{3+} , a tubular nanocomplex named OCNT@COF-Fe (O@CF) can be obtained, demonstrating outstanding photodynamic activity in generating ROS. The covalent crosslinking of the COF coating allows this complex to be uniformly dispersed within a Schiff base hydrogel, resulting in an antimicrobial, injectable (Fig. 5A(b)), conductive hydrogel (O@CF@G hydrogel) (Fig. 5A(c)) that is suitable for wound healing applications.⁶⁸

In a recent study, CNTs were incorporated into methyl acrylate crosslinked GelMA hydrogels using a rotating liquid bath electrospinning technique, producing oriented conductive hydrogel fibers. These hydrogel fibers exhibit microscale arrangements that simulate the structure of neuronal axons, electrical conductivity, and soft mechanical properties, holding great promise for applications in neural tissue engineering.⁶⁹ Moreover, recent research has uncovered that a bucky gel can be obtained by mixing ionic liquids with CNTs through a simple mechanical milling, resulting in a network of CNT frameworks filled with a large amount of ionic liquid. The entangled bundles of CNTs are broken into smaller bundles, creating a permeation network within the ionic liquid. This CNT network can then be transferred to a hydrogel matrix *in situ* by polymerizing suitable monomers in the ionic liquid, followed by solvent replacement with polyethylene glycol to create a CNT-hydrogel composite material.⁷⁰ It is a convenient and effective protocol for creating conductive hydrogels, suitable for future applications in tissue engineering.

Graphene oxide (GO) and reduced GO (rGO), alongside CNTs, serve as prevalent carbon-based materials in the preparation of conductive hydrogels.⁷¹ Current empirical evidence suggests that GO in Fig. 5B, serving as a functional additive, can thwart the progression of the Knoevenagel condensation reaction between benzaldehyde and cyanoacetate group-functionalized dextran polymers. Under conditions where a dextran hydrogel has not yet formed upon the introduction of histidine into this mixture, the solution undergoes a rapid sol-gel transition, forming a hydrogel endowed with conductive properties (Fig. 5B(a)). This hydrogel boasts superior electrical conductivity, translating human motion into resistive signals. Its pronounced responsiveness and advantageous electrical properties align well with microfluidic 3D printing technologies. Consequently, this conductive hydrogel is considered a viable 3D print medium (Fig. 5B(b)), poised to play a pivotal role in minimally invasive *in vivo* bioprinting, facilitating accurate tissue formation and repair.⁷² An additional study involved the self-assembly of agarose microbeads coated with GO into a granular hydrogel, which, with gentle heat, transformed into a conductive hydrogel containing a 3D network of reduced GO. This hydrogel boasted high electrical conductivity, low impedance, and elastic properties reminiscent of soft tissues, which can be easily shaped into various conductive structures through molding and 3D printing.⁷³

The most recent study developed a conductive polyacrylamide/sodium alginate cross-linked hydrogel containing rGO, exhibiting antibacterial, anti-inflammatory, and antioxidant properties. This hydrogel was capable of converting the “short circuit” at the site of injury into a “complete circuit”, thereby prompting fibroblasts near the wound to secrete growth factors, accelerating tissue regeneration.⁷⁴ Rapid advancements in the field of two-dimensional nanomaterials are being driven by the MXene family (the booming transition metal carbides, nitrides, and carbon nitrides), which are highly coveted for their metallic conductivity, extensive aspect ratio, solution processability and versatile tunability.⁷⁵ These attributes position them as an enthralling multifunctional platform for conductive hydrogels for tissue repair applications.^{76,77} An example includes the rapid formation of a hydrogel by blending phytic acid (PA), polyvinyl pyrrolidone (PVP), and MXenes in optimal ratios. PA serves as a crosslinker, establishing hydrogen bonds with the PVP polymer matrix to facilitate the development of a 3D physical crosslinking network. The reversible hydrogen bonds contribute to the hydrogel's excellent injectability and self-healing properties, while the integration of MXenes enhances its conductivity.⁷⁸ In another study shown in Fig. 5C, an antioxidant and conductive hydrogel was prepared by embedding MXene nanosheets (Ti_3C_2) into a temperature-sensitive ECM hydrogel. This hydrogel exhibited significant antioxidant and conductive properties and was capable of effectively neutralizing ROS.⁷⁹ Similarly, the two-dimensional titanium carbide ($\text{Ti}_3\text{C}_2\text{T}_x$) MXene, when mixed with Gel and dextran aldehyde (dex-ald), has been innovated into a conductive adhesive hydrogel capable of effectively restoring a variety of electrically active tissues, including the heart, muscles, and nerves.⁸⁰ It is evident that most MXene

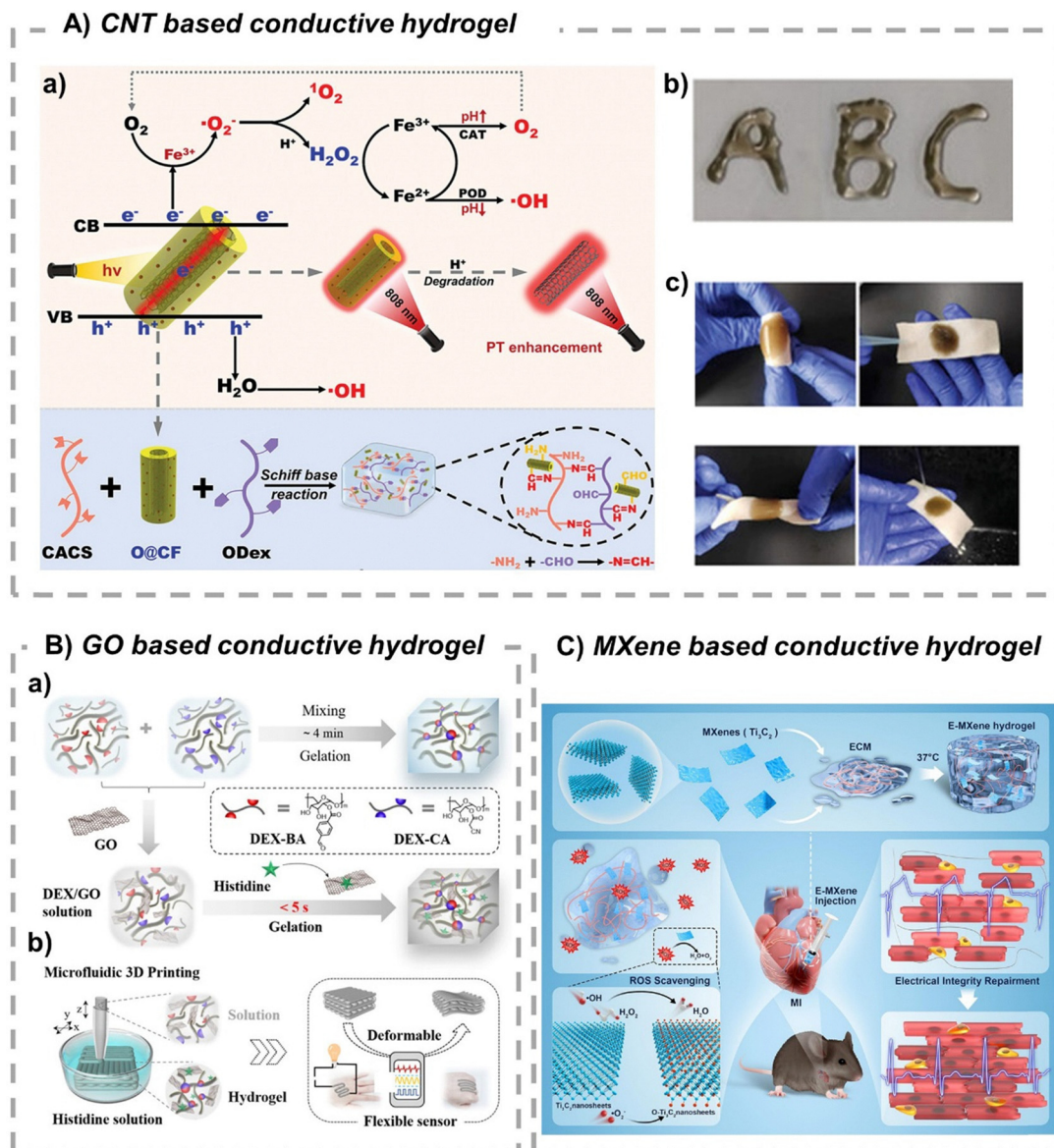


Fig. 5 Conductive hydrogels based on Carbon-Based Nanomaterials. (A) CNT-based conductive hydrogel. (a) Mechanisms for the ROS/O₂ generations and photothermal enhancements of O@CF and illustration for preparing O@CF@G hydrogel. (b) Photographs of the injectable O@CF@G hydrogel through the 22 G needle. (c) Photographs of the adhesions of O@CF@G to pig skin under bending, warping, water washing, and air blowing, respectively. Reproduced from ref. 68 with the permission of Wiley-VCH GmbH, copyright 2024. (B) GO-based conductive hydrogel, schematic diagram of the DEX/GO hydrogel fabrication, and use as a 3D printable polymer ink. (a) Gelation process of the DEX solution in the presence or the absence of GO in the histidine solutions. (b) DEX/GO solution can be used as a 3D printable polymer ink, by which a free-standing and deformable scaffold could be prepared through the microfluidic 3D printing technique when the DEX/GO solution was injected into the histidine solution (left); the printed construct could be further used as a flexible sensor (right). Reproduced from ref. 72 with the permission of American Chemical Society, copyright 2022. (C) MXene-based conductive hydrogel, schematic illustration of the preparation and application of E-MXene hydrogel. Reproduced from ref. 79 with the permission of Elsevier, copyright 2024.

hydrogels reported are based on Ti₃C₂T_x, which is the most advanced in terms of the synthesis and property study within the MXene family. However, this also means ample room for improvement in the targeted applications of hydrogels derived from MXene materials. The conductive hydrogels based on carbon-based conductive materials have reached a high level of development. However, these materials may pose a risk of thrombosis in the body and are difficult to metabolize,

restricting their application in the medical and clinical fields. Most materials utilized for skin wound repair typically only contact a limited wound area, thereby eliminating the issues of metabolism and thrombosis risk. Nevertheless, carbon-based conductive hydrogels still hold significant potential for application in wound repair.

A comprehensive analysis reveals that conductive hydrogels, categorized by their distinct types, possess varying degrees of

Table 1 Conductivity and application of different conductive hydrogels

Conductive hydrogels	Representative material	Conductivity ($S\ m^{-1}$)	Field of application
Conductive polymers based	PEDOT:PSS-based	2×10^3	3D printing, with potential for wearable and implantable applications ³⁴
Metal nanomaterials based	PPy-based	2×10^{-1}	Promote the repair of spinal cord injuries ⁴⁰
	PANI-based	$8.27 \pm 0.37 \times 10^{-2}$	Repair of peripheral nerve injury ⁴⁵
	Au-based	$2-4 \times 10^{-3}$	Parkinson's disease treatment ⁵¹
Ionic conductive hydrogels	Ag-based	7×10^{-2}	Human-machine electronics ⁵⁹
Carbon-based nanomaterials based	TA/HLC/PVA	1×10^{-5} – 2.6×10^{-1}	Deep wound treatment ²²
	CNTs-based	1.2×10^{-1}	Diabetic wound healing ⁶⁸
	GO-based	$1.5-5 \times 10^{-4}$	3D printing ⁷²
	MXene-based	5.29×10^{-3}	Myocardial infarction treatment ⁷⁹

conductivity and application scope. Table 1 provides an orderly and precise summary of these findings.

Applications of conductive hydrogels for wound healing

Upon skin injury, the positive charges within the wound interact with the negative charges surrounding the entire skin to generate an endogenous EF that aids in the migration of cells involved in wound healing. Consequently, ES is an adjunct method that can facilitate the seamless transfer of these endogenous EF charges. However, the bulk of external ES devices often hinders their ability to conform perfectly to the wound, necessitating the development of flexible conductive hydrogels that can cover the wound site and effectively transmit electrical signals. Conductive hydrogels have emerged as a focal point in the field of wound healing, with various types being developed to cater to different wound presentations.^{81,82}

Acute wounds

Acute wounds are typically defined as injuries that occur suddenly, including surgical cuts and second-degree burns. Their healing generally begins in the first phase of the wound healing process, known as the hemostatic phase. This stage primarily involves tissue regeneration through the collaborative efforts of platelets, fibroblasts, and microcells. Generally, acute wounds require 8 to 12 weeks to heal, while larger or open wounds often cannot close through self-contraction, making healing difficult. Therefore, accelerated wound healing is crucial in the healing process of acute wounds.

Research indicates that electrical stimuli promote wound healing with high efficacy and a low incidence of side effects. An instance (Fig. 6A) can be observed with a conductive hydrogel synthesized using silver nanowires (Ag-NW) and methacrylated alginate (MAA), which is capable of being printed onto medical-grade dressing patches (e-patch) (Fig. 6A(a) and (b)). Such hydrogels effectively stimulate re-epithelialization and enhance vascular formation within a wound's microenvironment. ES increases the output of growth factors (Fig. 6A(c)), resulting in elevated cell proliferation and migration rates. Within 18 hours, the fibroblasts in the ePatch group with an EF, denoted as ePatch w/EF, exhibited a significantly faster migration rate than those in the ePatch group without an EF, and showed a higher migration efficiency. (Fig. 6A(d)). Animal testing demonstrates that, compared to the standard 20-day

healing duration in rodents, wounds treated with this hydrogel heal significantly faster, often within 7 days (Fig. 6A(e) and (f)). During the experimental period, no significant improvement in wound healing was observed in either the control group or the ePatch group by the fourth day. However, in the ePatch w/EF group, a noticeable closure of the circular wound occurred vertically, resulting in only a minor residual wound area. Consistent with the outcomes of the *in vitro* migration assay, the promotion of wound closure was exclusively observed in the ePatch w/EF group. This trend of rapid wound healing persisted throughout the experiment, up to the seventh day, with a linear wound bed evident only in the ePatch w/EF treated group. Moreover, due to irregular tissue regeneration processes, the wound edges in both the control group and the ePatch group remained circular and wrinkled-like, whereas the wound edges in the ePatch w/EF group were nearly linear. The control group's wound area measurements were $57.9 \pm 3.3\%$ on day 4 and $31.4 \pm 7.5\%$ on day 7. In the ePatch group, they were $57.1 \pm 4.0\%$ on day 4 and $28.6 \pm 4.6\%$ on day 7; and in the ePatch w/EF group, they were $25.7 \pm 1.3\%$ on day 4 and $9.8 \pm 4.5\%$ on day 7.⁴⁸ For deeper wounds, conventional hydrogels only cover the exposed area, leaving a cavity behind and presenting certain limitations. However, the novel ionic hydrogel introduced in the text above, which integrates TA and HLC into the PVA and borax hydrogel network, can autonomously conform to the contours of deep wounds, effectively overcoming these limitations and offering an excellent treatment option for such deeply penetrating injuries. Adaptive conductive hydrogels can seamlessly adapt to deep wound cavities, allowing for the transmission of both native and externally applied electrical currents. This promotes intercellular signaling as well as the distribution of exogenous electrical stimuli, enhancing cell migration and blood vessel formation. Among them, the cell proliferation rate was notably higher on scaffolds subjected to ES than in the control group. The cell growth in the groups receiving ES was substantially greater than in the untreated (no ES) groups for the conductive hydrogels in question. In animal trials, complete wound closure was achieved by day 10, with reconstitution of the subdermal tissue, including blood vessels and hair follicles, greatly expediting wound healing. In the study, by the 10th day, the wound healing rate in the control group reached only 50%, while the control + ES group achieved a healing rate of 62%. Conversely, the wound healing rate for the group

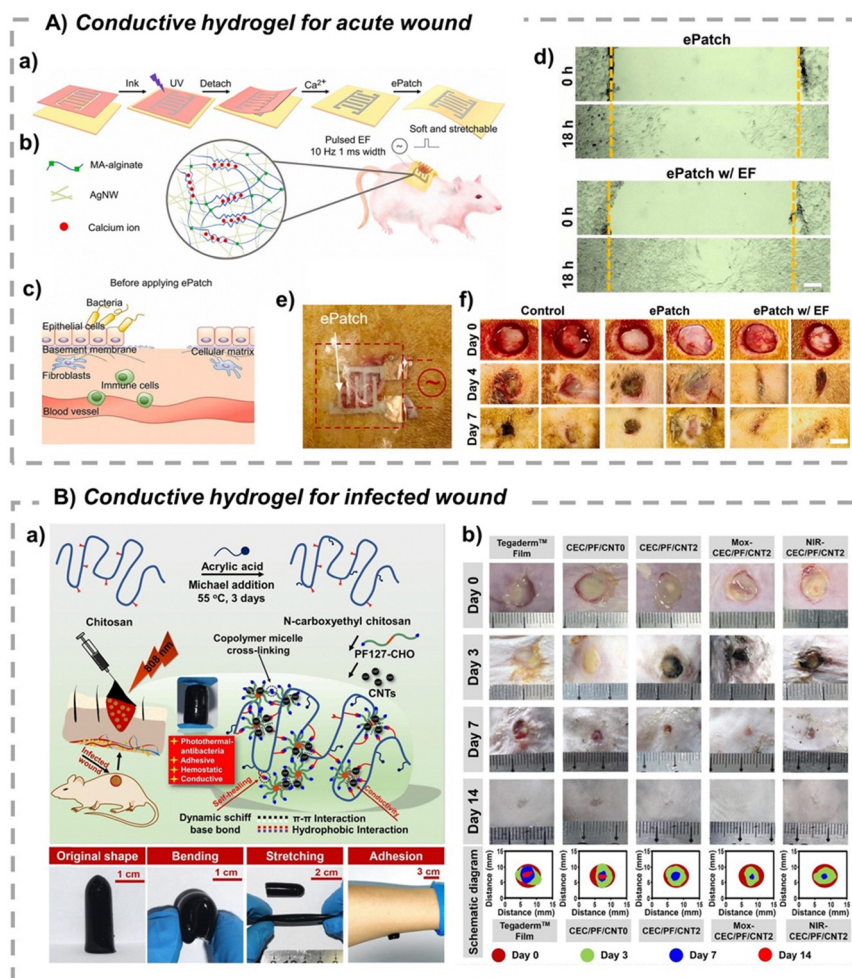


Fig. 6 (A) Conductive hydrogels for acute wounds. (a) Schematic of the ePatch fabrication. (b) Schematic of the Ag-NW-MAA ink formula and the double-crosslinked network. (c) Illustration of the biological activities of the ePatch during the healing process. (d) Microscopic images of the scratch assay. Cells were stimulated with or without EF. (e) Photograph of the ePatch applied on the back of an SD rat. (f) Optical images of wounds and residual wound areas in different groups at days 4 and 7. Reproduced from ref. 48 with the permission of Elsevier, copyright 2022. (B) Conductive hydrogels for infected wounds. (a) Schematic representation of the CEC/PF/CNT hydrogel preparation: original shape, bending, stretching shape representations, and adhesion behavior of the CEC/PF/CNT2 hydrogel. (b) Photographs and schematic diagrams of the wound closure on the 3rd, 7th, and 14th day. Reproduced from ref. 92 with the permission of Elsevier, copyright 2020.

treated with the hydrogel dressing alone was between 69% and 72%. Notably, the conductive hydrogel + ES group wound had completely closed by the 10th day, exhibiting only minimal scarring. The combination of the hydrogel and ES demonstrated a synergistic effect that significantly enhanced the rate of tissue regeneration.²² Furthermore, an injectable self-healing hydrogel with biomechanical activity, based on quaternized chitosan (QCS), polydopamine-coated rGO (rGO-PDA), and poly(*N*-isopropylacrylamide) (PNIPAm), has been developed. They firmly adhere to the skin, actively constrict wounds through self-contraction to aid in healing, and possess good self-healing properties, temperature-dependent drug release capabilities, antibacterial effects, antioxidant properties, and conductivity. *In vivo* full-thickness skin defect models have indicated that hydrogel dressings significantly promote wound closure, accelerate wound contraction, and facilitate the healing process of the wound site, with increased granulation

tissue thickness, enhanced collagen distribution, and improved vascularization.⁸³

Chronic wounds

Chronic wounds typically arise from various factors following trauma, including the development of bacterial biofilms,⁸ or are caused by conditions such as aging, chemotherapy, radiotherapy, immunosuppression, and systemic malignancies such as diabetes,⁶ which impede proper wound healing and are generally classified into two main types: infectious wounds and diabetic wounds.

Infected wounds

The antimicrobial activity is vital for the healing of infected wounds, and antimicrobial dressings are a commonly employed strategic intervention. The inherent properties of hydrogels make them suitable matrices for the delivery of antibiotics,

with numerous antibiotics and antimicrobial agents encapsulated within conductive hydrogels to create local, drug-resistant, and sustained-release systems. These systems effectively control bacterial proliferation in skin wounds and promote healing. Moreover, metals, carbon-based materials, conductive polymers, ionic compounds, and other substances that impart conductivity to hydrogels also enhance their antimicrobial properties. For example, the photothermal properties of CNTs^{84–86} and PPy,^{87,88} as well as the photothermal antibacterial properties of GO,^{84,89–91} enhance the healing of infected wounds.

The self-healing conductive antibacterial hydrogel, made from a material blend of oxidized sodium alginate grafted with dopamine, CMCS, and Fe³⁺, encapsulated within PPy-3-acetic acid, exhibits commendable conductivity, photothermal antibacterial activity, and antioxidant capabilities when exposed to near-infrared (NIR) light. In the study of infected full-thickness skin wound repair in mice, the conductive hydrogel improved healing efficacy in infected wounds when combined with NIR irradiation. After 14 days, the wound area decreased by 12% compared to commercially available Tegaderm™ dressings. The thicknesses of the vascular tissue, hair follicles, and epidermis approached normal skin levels. Inflammation diminished, and the granulation tissue became thicker.³ Similarly, due to the photothermal antibacterial properties of the material, the conductive self-healing adhesive hydrogel, fabricated from benzaldehyde-terminated Pluronic F127/CNTs and *n*-carboxyethyl chitosan (CEC/PF/CNT hydrogel), has been validated *in vivo* to possess significant potential as a photothermal therapy (PTT) material for treating infected wounds (Fig. 6B). It effectively enhances wound healing (Fig. 6B(b)), collagen deposition, and angiogenesis, indicating promising therapeutic prospects for managing infected wounds.⁹²

Furthermore, satisfactory healing of chronic wounds associated with multidrug resistant (MDR) bacterial infections remains a significant challenge due to persistent inflammation and severe bacterial pathogenesis. In the context of chronic wounds infected with methicillin-resistant *Staphylococcus aureus* (MRSA), typical MDR bacteria, carbonitride (Nb₂C) MXene materials have shown remarkable antioxidant properties. Accordingly, a study utilized Pluronic F127 aldehyde (FCHO), branched polyglycerol-amino acid (GEPL), PDA modified Nb₂C MXene nanosheets (Nb₂C@PDA), and 3,3'-dithiodipropionic acid (DTPH) to prepare a conductive hydrogel through a Schiff base reaction. This hydrogel effectively scavenges excessive ROS and demonstrates 100% *in vitro* antibacterial efficiency against MDR MRSA. It significantly accelerates the healing of MRSA-infected wounds by promoting rapid hemostasis, eradicating bacterial infections, exhibiting anti-inflammatory effects, stimulating cell proliferation, angiogenesis, granulation tissue formation, collagen deposition, and re-epithelialization, achieving a healing rate up to 97.3%.⁹³

In another study, a conductive hydrogel based on an ionic liquid containing Zn²⁺ was synthesized through multiple bound crosslinking, exhibiting good cell compatibility and antioxidant properties. Integrating Zn²⁺ into the hydrogel

provided significant bacteriostatic effects against MRSA and *E. coli*. The healing effect of the hydrogel on MRSA-infected mouse neck skin wounds was confirmed, showing improvements in the wound healing rate, collagen deposition, and granulation tissue thickness due to reduced inflammation and enhancement angiogenesis.⁹⁴ Additionally, in a classic study previously mentioned, researchers innovatively combined titanium carbide Ti₃C₂T_x MXenes with the antioxidant cerium dioxide (CeO₂) to fabricate conductive hydrogels. This novel conductive hydrogel not only continues the photothermal antibacterial characteristics of the MXenes but is also infused with the antioxidant capabilities of CeO₂. This integration plays a significant role in alleviating the inflammatory responses encountered in the early stages of wound healing. Moreover, in the cell proliferation experiment, the conductive hydrogel scaffold combined with ES yielded a significantly higher cell count than the other groups, suggesting that conductivity is an effective stimulator of cell proliferation. Moreover, the scratch assay results revealed a marked decrease in the non-healing rates of scratches, with the control group, electrode group, and hydrogel-ES group exhibiting rates of 59.6%, 50.3%, and 48.2%, respectively. Particularly striking was the closure rate of the scratches in the group treated with a combination of conductive hydrogel and ES, which reached an impressive 73.6% within 24 hours, thereby conclusively demonstrating the substantial promotion of cell migration by this combined approach. The hydrogel's conductivity can efficiently promote granulation tissue formation, blood vessel regeneration, collagen deposition, and re-epithelialization, contributing materially to the accelerated treatment and healing of MDR infected wounds.⁷⁶

While the photothermal antibacterial function of most conductive materials plays a significant role in treating infectious wounds, it is crucial to recognize the potential for secondary skin damage caused by short-term high temperatures. Therefore, intelligent temperature control on the wound surface remains an area that requires further exploration. Antibacterial and infection control are merely components in skin wound repair. Effective wound repair demands the coordination of additional steps and processes and enhancements in the real-time monitoring capabilities of conductive hydrogels for assessing the degree of bacterial infection on the wound surface.

Diabetic wounds

Diabetes is a multifaceted metabolic disorder, and chronic wounds represent one of the most serious complications of this condition. Approximately 25% of patients with diabetes will require amputations, and at least 68% of these individuals will not survive beyond five years following their amputation. The hallmarks of these wounds include elevated levels of ROS, a consequence of chronic hyperglycemia, which lead to oxidative stress, diminished antioxidant defenses, and the production of free radicals. This ultimately results in microvascular damage, inhibition of angiogenesis, and prolonged inflammation.⁹⁵

Metformin, a widely employed agent in diabetes management, exerts significant protective effects on microvessels within a hyperglycemic environment. It achieves this by

enhancing mitochondrial autophagy, which reduces endothelial cell damage caused by high glucose levels. Additionally, metformin activates the AMPK signaling pathway in vascular endothelial cells and inhibits the activity of NF- κ B, a regulatory protein that promotes inflammation. By doing so, it down-regulates the expression of pro-inflammatory cytokines and adhesion molecules, contributing to preserving vascular integrity and function. Exosomes can transport proteins, mRNA, miRNA, and other small molecular substances to target cells, triggering signaling cascades that promote tissue regeneration. By reducing the production of ROS, they can alleviate oxidative stress-related skin damage, thereby decreasing DNA damage, mitochondrial alterations, histopathological injuries, and inflammation.

Studies have explored the crosslinking and coordination of four-arm SH-PEG with Ag⁺ to create PEG hydrogels, along with the combination of hydroxyl-modified multi-walled CNTs through disulfide bonds to form hydrogen bonds, ultimately resulting in a stable, conductive 3D structure. Using metformin as a model drug and ADSCs-Exos as bioactive substances, the highly interconnected porous network formed by the coordination crosslinking method effectively mobilizes and releases metformin and exosomes for treating diabetic wounds. The wound-healing efficacy of this conductive hydrogel is attributed to its ability to protect the integrity and barrier properties of the microvasculature, quell inflammation, and enhance cell proliferation and the formation of new blood vessels. It operates by disrupting mitochondrial fission, reducing the generation of mtROS and cellular ROS, and it shields the stability of F-actin amidst hyperglycemic states.⁹⁶ Researchers have fabricated a dually responsive hydrogel that can release metformin by pH and glucose levels. L-Arginine was incorporated to introduce cationic antimicrobial activity, and reduced rGO coated with PDA (rGO@PDA) endowed the material with conductivity and hemostatic capabilities. The hydrogel facilitates the healing of type II diabetic foot ulcers by decreasing inflammation and promoting blood vessel formation. The combined effect of rGO@PDA's conductivity and the pharmaceutical action of metformin further improved the healing rate of diabetic wounds.⁹⁷ Chronic inflammation in diabetic wounds is not solely a consequence of oxidative stress and impaired vascularization but is also significantly influenced by the overabundance of MMPs and inflammatory mediators induced by persistent high glucose levels. To combat these challenges, scientists have developed a nanogel system featuring TA conjugated with siRNA that self-assembles and crosslinks with PVA, HLC, and TA, with borax added for structural reinforcement, named PHTB(TA-siRNA) hydrogels (Fig. 7A(a)). This hydrogel can release the nanogel under oxidative stress, directly targeting and reducing MMP-9 expression. TA and HLC simultaneously drive collagen synthesis, reduce inflammation, and lower ROS levels. Additionally, ES of the hydrogel enhances the release of the nanogel within the body, promoting optimal macrophage behavior, increased collagen production, and angiogenesis, which are crucial for the healing of diabetic ulcers (Fig. 7A(b)). For example, within a diabetic rat model

exhibiting full-thickness skin defects, the diabetic rats treated with a combination of ES and PHTB hydrogel demonstrated complete wound healing by the 10th day. In contrast, the control group of diabetic rats reached complete healing on the 19th day. The integration of ES therapy with the PHTB hydrogel (enhanced with TA-siRNA) resulted in a 47.4% reduction in the healing time for the diabetic rats' full-thickness skin defects, thereby markedly improving the efficacy of wound repair.²¹

Conductive hydrogels with antioxidant and anti-inflammatory capabilities have been widely employed to repair diabetic wounds. Nonetheless, the inflammatory stage and ROS are also indispensable in wound healing. Excessive reduction of inflammation levels can hinder wound healing, while ROS can coordinate the recruitment of lymphocytes, mediate the defense of phagocytes, inhibit bacteria, and regulate wound angiogenesis. Unreasonably eliminating ROS and inflammation is detrimental to wound healing. It can be seen from this that achieving controllability of ROS levels is a problem that should be considered in the repair of diabetic wounds and even all wounds, and it is also the development prospect of conductive hydrogels in the field of wound repair.

Wound monitoring

Through the research above, we have comprehensively understood the complexity of skin wound repair and the variability in recovery status. Consequently, real-time monitoring of various trauma indicators is essential for medical staff and clinical treatment. It allows them to stay informed about the wound's physiological state, assess the current treatment's effectiveness, and adjust the treatment plan as necessary. Moreover, it enables early detection of potential issues with the wound.

In the context of the broad application of conductive hydrogels in biosensors,⁹⁸ a series of conductive hydrogels that can monitor the physiological status indicators of wounds while simultaneously promoting wound healing have been developed. For example, the temperature at the wound site is highly correlated with inflammation, infection, blood supply, and other factors. During the process of wound healing, inflammation, inflammation factor-induced vasodilation, and immune responses can cause an increase in the temperature of the skin wound tissue, which is approximately 1.5 °C higher than that of normal skin temperature.^{99,100} Therefore, monitoring the temperature during wound healing management can promptly reflect the condition of the wound. In addition to temperature, continuous motion monitoring based on strain is also significant for stubbornly mobile wounds that frequently deform, such as joint wounds. Additionally, pH, glucose concentration, lactic acid concentration, and inflammatory cytokine levels can all be tracked as markers reflecting the physiological state of the wound.

In one of the recent studies, a novel multifunctional conductive hydrogel patch has been proposed, drawing inspiration from various organisms such as octopuses and snails (Fig. 7B). It consists of tannin-grafted Gel, Ag-tannin NPs, polyacrylamide (PAAm), and poly-N-isopropylacrylamide (PNIPAm), featuring

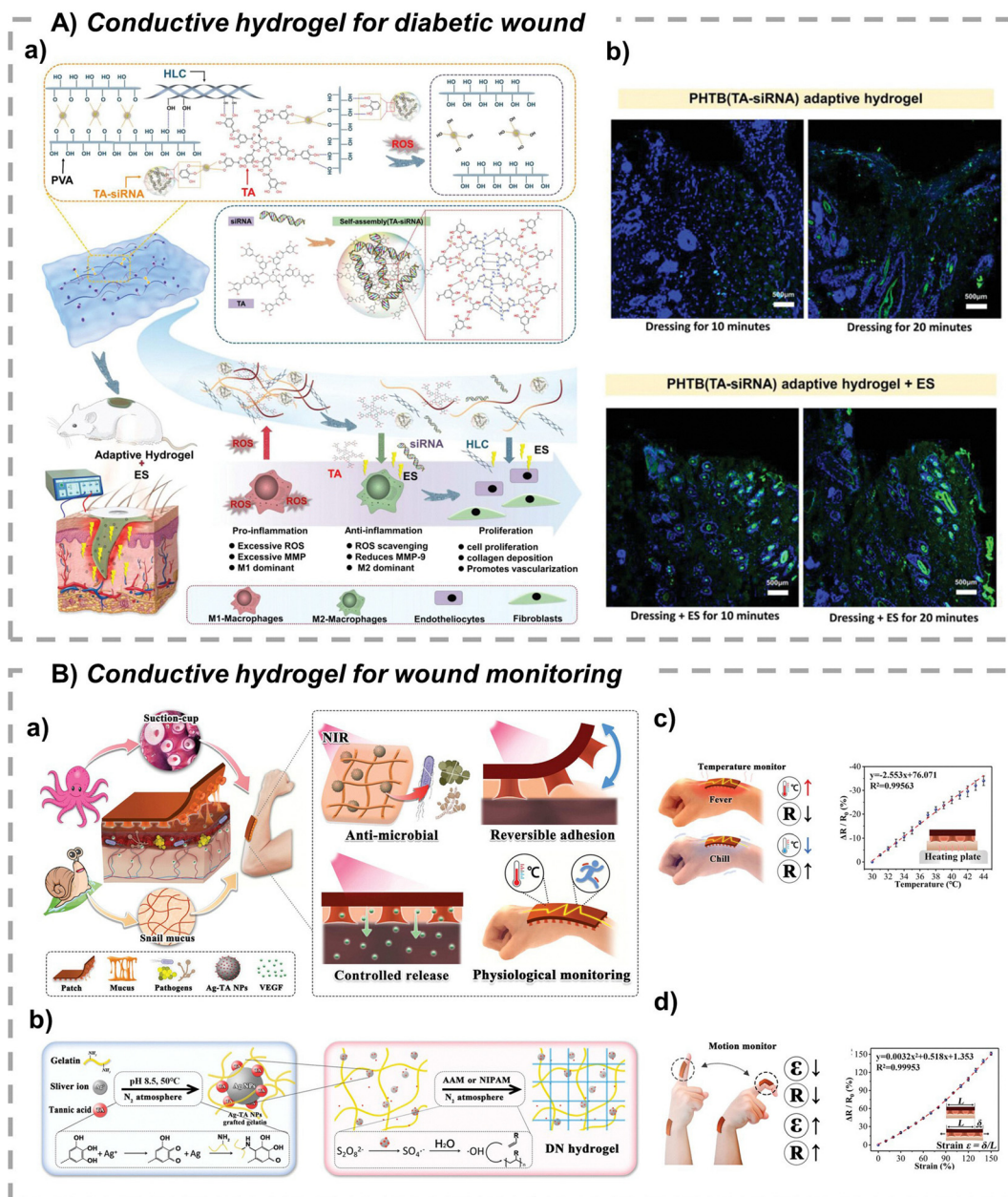


Fig. 7 (A) Conductive hydrogels for diabetic wounds. (a) The repair of diabetic chronic wounds using the combination of ES therapy and adaptive, conductive PHTB(TA-siRNA) hydrogels. (b) Effect of ES therapy on the release of siRNA from PHTB(TA-siRNA) hydrogels during wound application. The siRNA was labeled with a green immunofluorescent stain (i.e., 5-FAM), and the blue color represents DAPI-stained nucleus. Reproduced from ref. 21 with the permission of Wiley-VCH GmbH, copyright 2022. (B) Conductive hydrogels for wound monitoring. (a) Schematic diagram of multi-bioinspired functional hydrogel patches for wound healing management. (b) Schematic diagram of mucus, PAAm-DN, and PNIPAm-DN synthesis. (c) Continuous sensing of temperature and resistance change rate ($\Delta R/R_0$), temperature curve of the patch. (d) Continuous monitoring of motion by the patch and the resistance change rate ($\Delta R/R_0$) strain curve of the patch. Reproduced from ref. 101 with the permission of Wiley-VCH GmbH, copyright 2023.

controllable adhesion, antibacterial properties, and drug release functions (Fig. 7B(b)). The excellent conductivity of TA-Ag NPs, combined with the stability and adhesion of the hydrogel, allows this patch to provide flexible, continuous, and stable monitoring compared to traditional devices. This patch can monitor temperature by tracking changes in resistance (Fig. 7B(c)). Within the body temperature range of 30 to 44 °C, the temperature coefficient of resistance is $-2.43\% \text{ } ^\circ\text{C}^{-1}$, indicating the sensitivity of the

monitoring and its ability to reflect real-time temperature changes of the wound. Moreover, the resistance change rate of this patch can reach 86% under 100% strain, with a strain coefficient of 0.85966, which indicates that the patch has good sensitivity and a broad monitoring range, making it suitable for monitoring joint wounds (Fig. 7B(d)). At the same time, the photothermal gel-sol transition of tannin-grafted Gel and Ag-tannin NPs gives the patch a dual antibacterial effect. Moreover, the “suction cup” composed

of thermoresponsive PNIPAm can undergo contraction–relaxation transformation, allowing the medical patch to reversibly and responsively attach to the object and controllably release the vascular endothelial growth factor (VEGF) it carries, thereby promoting wound healing.¹⁰¹

Another study reveals that the nanocomposite conductive hydrogel made from 3-acrylamidophenylboronic acid (APBA) and acrylamide (AM), synthesized in the presence of LAPO-NITE[®] XLG nanosheets, stabilizes CNTs. Some weak non-covalent interactions within the network will dissociate upon heating, thereby enhancing the electron migration rate. Consequently, it possesses a temperature-sensing capability and can reflect local temperature changes of the wound through the resistance temperature coefficient, facilitating the monitoring of the skin wound healing process. The mouse wound temperature monitoring experiment successfully monitored the relative resistance differences at various stages of wound healing to detect temperature changes. At the same time, the conductive hydrogel can also promote wound healing.¹⁰² In addition to monitoring the state of the wound through temperature, another conductive hydrogel has been developed, which is prepared from chitosan quaternary ammonium salt (HACC) and sodium alginate (SA) as raw materials through blending and acid treatment. It has an arbitrary shape and high flexibility and can be applied to wounds with irregular shapes. Due to the presence of free Cl[−], the hydrogel exhibits excellent electrical conductivity. Its resistance change shows a positive linear relationship with the change in the area, indicating that the hydrogel can monitor changes in the wound area, provide information on these changes, and simultaneously promote collagen deposition and blood vessel formation, significantly enhancing wound healing.¹⁰³ Treating wounds at the joints is relatively complex because frequent movement causes the dressing to crack and become susceptible to bacterial infection, making it hard to adapt to and monitor irregular wounds.

A conductive hydrogel has emerged for application to wounds at the joint. This hydrogel is developed from polysaccharide biopolymers, PVA, and hydroxylated graphene (GOH) through dynamic borate ester bonds and supramolecular interactions, offering good electromechanical properties. When the wound is infected by bacteria, their growth, reproduction, and metabolism produce acidic compounds, leading to a gradual decrease in the pH of the microenvironment. Regarding this type of hydrogel, when the pH at the bacterial contact site drops below the pK_a of the phenylboronic acid group (approximately 8.5), the borate ester bond fractures, causing the hydrogel network to dissociate partially. This sol–gel transition accelerates electron flow in GOH, significantly reducing resistance and enabling bacterial detection. This conductive hydrogel can detect bacterial infections through variations in electrical signals, thus achieving real-time monitoring. It can harness the photothermal characteristics of hydroxylated graphene for *in situ* sterilization, effectively preventing the re-tearing of human joint wounds.¹⁰⁴

The biomimetic and sensing characteristics of conductive hydrogels can effectively monitor subtle changes in various

indicators during the wound healing process, and they have broad application prospects. Nevertheless, the current applications of the sensing characteristics of conductive hydrogels are mainly focused on motion monitoring, with fewer applications in wound repair. Moreover, some conductive hydrogels designed to monitor wound status, including parameters such as temperature, wound area, and exudate concentration, encounter challenges in accurately distinguishing specific change parameters. Therefore, developing conductive hydrogels that can be precisely applied to monitor various types of wounds remains a significant challenge.

Discussion and perspectives

This article reviews the recent research on conductive hydrogels in skin wound repair. Wound healing is a complex and dynamic process aimed at restoring missing cell structures and tissue layers, which can be divided into four stages: hemostasis, inflammation, proliferation, and remodeling. Through this summary, we have discovered that conductive hydrogels can exert their effects in different repair stages of the skin due to their diverse properties. During the hemostasis stage, conductive hydrogels can activate the coagulation pathway through their charges, accelerating hemostasis. This property is more prominently manifested in ionic hydrogels. Upon transitioning to the inflammatory stage, wounds face issues such as infection and excessive oxidation, making the need for anti-inflammatory, antioxidant, and antibacterial functions urgent. Conductive hydrogels can provide an antioxidant effect, thereby suppressing inflammation. At the same time, the photothermal properties inherent in most conductive materials give conductive hydrogels the ability to display photothermal antibacterial properties, allowing them to inhibit bacterial growth during the inflammatory stage effectively. In the subsequent proliferation phase, the endogenous EF and stimulating current generated by the conductive hydrogel through ES at the wound site can control the electrodrive of cell migration by influencing key signaling pathways (such as PI3K/Pten). For instance, it can affect the TGFβ1-ERK-NF-κB signaling pathway to promote the proliferation of fibroblasts, thereby enhancing wound contraction. At the same time, it can also stimulate endothelial cells to secrete VEGF factors, promoting angiogenesis through the PI3K-Akt and Rho-ROCK signaling pathways and accelerating collagen deposition. Ultimately, in the remodeling stage, the conductive hydrogel speeds up the maturation and remodeling of collagen, permeating the entire wound healing process. Compared with conventional wound dressings and other biocompatible materials, conductive hydrogels provide a moist microenvironment, replicate the ECM architecture, and exhibit enhanced drug loading capacity. In contrast to conventional hydrogels, conductive hydrogels introduce active ES, emulating the intrinsic EF within the body. This feature offers a synergistic effect in promoting angiogenesis and epithelialization, establishing a clear advantage for their application in wound healing.

As delineated in the introductory section, conductive hydrogels of various types display distinct characteristics in terms of their performance. For example, conductive hydrogels based on conducting polymers, predominantly employing materials such as PPy, PEDOT and PANI, achieve conductivity through chemical cross-linking or doping processes. Among these, self-healing capabilities are notably enhanced in dynamic bond systems, such as those utilizing TA cross-linking in PPy gels. However, PEDOT-based hydrogels exhibit limitations in self-healing due to their inherent rigidity. Regarding superelasticity, ionic and PPy gels incorporating dynamic bonds demonstrate exceptional deformation properties. Conversely, composite hydrogels containing PEDOT and CNTs exhibit reduced superelasticity due to the weaker elasticity of their rigid network. Surface chemistry predominantly influences adhesion properties, with systems incorporating PDA or TA demonstrating superior adhesion. Antimicrobial efficacy is strongly associated with the material composition: silver-based hydrogels and photothermal materials, such as PPy/CNT composites, exhibit significant antibacterial activity, whereas pure ionic gels generally exhibit weaker antimicrobial properties.

Despite the substantial potential exhibited by the conductive hydrogel in skin wound repair, the highly intricate nature of the skin wound repair process presents numerous challenges that remain to be overcome to achieve flawless repair.

First and foremost, significant limitations remain in the mechanical properties of conductive hydrogels that can be freely adjusted. Most conductive hydrogels used in wound repair have a fixed morphology and are often applied as dressings on the wound surface. However, when faced with deep or irregular wounds, they struggle to adapt, hindering wound closure and impacting the hydrogel's therapeutic effect. Thus, developing injectable and adaptive conductive hydrogels to accommodate wounds of various shapes is a promising research direction. Additionally, most conductive materials employed in synthesizing conductive hydrogels possess a certain level of toxicity. Metal NPs are commonly associated with potential cytotoxic effects, necessitating surface modification to minimize dissolution and enhance biocompatibility. Conducting polymer monomers can also exhibit residual toxicity and thus require improvements in polymerization processes and purity to mitigate these issues. Carbon-based conductive hydrogels, while offering unique properties, may pose a risk of thrombosis, leading to their focus on applications primarily targeted at local wound repair, and pose standard problems in clinical applications. Hence, enhancing the biocompatibility of conductive hydrogels to make them suitable for clinical transformation remains an urgent issue that requires resolution. Future conducting hydrogels should emphasize biodegradable design and the preferential use of natural polymer-based materials, such as by incorporating PPy NPs with Gel or HA to enable natural metabolism within the body without accumulation, or by employing more chitosan, alginate, and other natural polymers as the base materials.

Furthermore, the application of intelligent dressings in skin wound repair offers considerable prospects for development.

For instance, monitoring wound conditions can reflect real-time variations in wound healing, thereby enabling the formulation of targeted treatment regimens. However, the use of conductive hydrogels in wound status monitoring is still in its infancy and exploration stage, mainly focusing on motion monitoring, and is often a simple combination of sensors and hydrogels. Monitoring physiological markers such as wound temperature, pH value, and glucose concentration is relatively scarce, and it is impossible to simultaneously track changes in multiple parameter indicators, which limits clinical applications. Accordingly, developing the multifunctionality and monitoring sensitivity of conductive hydrogels as wound monitoring materials is essential, which will establish the foundation for the future development of intelligent dressings that incorporate monitoring, analysis, and treatment. In response to the current limitations of intelligent hydrogels in their multi-parametric synchronous detection capabilities and the absence of a treatment feedback loop and to focus on future research endeavors, the objective is to establish and enhance a comprehensive treatment feedback loop system with rigorous scientific methodology and smooth operation. Finally, apart from monitoring the wound conditions, whether intelligent conductive hydrogels can be utilized in regulating and feedback inflammation also holds significant research and discussion value. Previous studies indicate that the inflammatory period is a critical stage in wound healing, where both inadequate and excessive inflammation can result in prolonged non-healing of the wound. Nonetheless, most conductive hydrogels facilitate healing through anti-inflammation during this stage, often overlooking that overly low inflammation can also hinder wound healing. Consequently, intelligent monitoring or regulation of inflammation *via* conductive hydrogels presents an auspicious direction for development.¹⁰⁵

Conclusion

This review paper summarizes the types of conductive hydrogels developed in recent years and their applications in skin wound repair. It discusses their advantages, limitations, and potential future development directions. Although the application of conductive hydrogels in skin wound repair is still in its infancy, it has seen remarkable growth recently. Overall, conductive hydrogels can enhance cell connection through ES, promote cell migration, adhesion, and proliferation, and stimulate the secretion of related factors, thereby facilitating wound healing. Additionally, by combining the properties of different hydrogels and conductive materials, conductive hydrogels provide dressings with additional functions, such as antibacterial, anti-inflammatory, adaptive, and injectable properties, which can be applied in treating various types of wounds. However, skin wound repair is a complex process that involves severe difficulties and challenges. Further investigation is needed into the mechanisms of conductive hydrogels in wound repair and the relationship between conductive hydrogels and ES to develop a more effective conductive hydrogel and achieve optimal repair of skin trauma.

Conflicts of interest

All authors declare that there are no competing interests.

Data availability

The authors confirm that the data supporting the findings of this study are available within the article.

Acknowledgements

This work was supported by the Natural Science Foundation of Shandong Province (ZR2024MH163), Qingdao Key Health Discipline Development Fund (2025–2027), and Shandong Provincial Key Medical and Health Discipline of Oral Medicine (2025–2027).

References

- J. Li, F. Yu, G. Chen, J. Liu, X.-L. Li, B. Cheng, X.-M. Mo, C. Chen and J.-F. Pan, *ACS Appl. Mater. Interfaces*, 2020, **12**, 2023–2038.
- M. Wang, Y. Luo, T. Wang, C. Wan, L. Pan, S. Pan, K. He, A. Neo and X. Chen, *Adv. Mater.*, 2021, **33**, 2003014.
- L. Qiao, Y. Liang, J. Chen, Y. Huang, S. A. Alsareii, A. M. Alamri, F. A. Harraz and B. Guo, *Bioact. Mater.*, 2023, **30**, 129–141.
- L. Qi, C. Zhang, B. Wang, J. Yin and S. Yan, *Macromol. Biosci.*, 2022, **22**, 2100475.
- R. Luo, J. Dai, J. Zhang and Z. Li, *Adv. Healthcare Mater.*, 2021, **10**, 2100557.
- H. Q. Tran, S. M. S. Shahriar, Z. Yan and J. Xie, *Adv. Wound Care*, 2022, **12**, 399–427.
- C. Attinger and R. Wolcott, *Adv. Wound Care*, 2012, **1**, 127–132.
- Y. Liang, H. Xu, Z. Li, A. Zhangji and B. Guo, *Nano-Micro Lett.*, 2022, **14**, 185.
- S. Barrientos, H. Brem, O. Stojadinovic and M. Tomic-Canic, *Wound Repair Regen.*, 2014, **22**, 569–578.
- J. G. Powers, C. Higham, K. Broussard and T. J. Phillips, *J. Am. Acad. Dermatol.*, 2016, **74**, 607–625.
- X. Qi, E. Cai, Y. Xiang, C. Zhang, X. Ge, J. Wang, Y. Lan, H. Xu, R. Hu and J. Shen, *Adv. Mater.*, 2023, **35**, 2306632.
- S. Ellis, E. J. Lin and D. Tartar, *Curr. Dermatol. Rep.*, 2018, **7**, 350–358.
- S. T. Haque, S. K. Saha, M. E. Haque and N. Biswas, *Biomater. Sci.*, 2021, **9**, 7705–7747.
- N. Liu, Z. Zhou, X. Ning, X. Zhang, Q. Guo, M. Guo, Y. Wang and T. Wu, *Mater. Des.*, 2023, **225**, 111582.
- Z. Zhou, Y. Wang, N. Liu, X. Zhang, X. Ning, Y. Miao, C. He, T. Wu and X. Leng, *Mater. Des.*, 2025, **253**, 113929.
- J. Wang, Z. Zhou, X. Zhang, M. Fu, K. Fang, Y. Wang and T. Wu, *Adv. Fiber Mater.*, 2025, **7**, 1148–1164.
- Y. Zhang, Z. Zhou, N. Liu, J. Wang, Q. Guo, Y. You, K. Mao, Y. Wang, W. Zhang and T. Wu, *J. Nanobiotechnol.*, 2025, **23**, 455.
- Y. Xiong, Z. Lin, P. Bu, T. Yu, Y. Endo, W. Zhou, Y. Sun, F. Cao, G. Dai, Y. Hu, L. Lu, L. Chen, P. Cheng, K. Zha, M.-A. Shahbazi, Q. Feng, B. Mi and G. Liu, *Adv. Mater.*, 2023, **35**, 2212300.
- Y. Qian, Y. Zheng, J. Jin, X. Wu, K. Xu, M. Dai, Q. Niu, H. Zheng, X. He and J. Shen, *Adv. Mater.*, 2022, **34**, 2200521.
- G. D. Winter, *Nature*, 1962, **193**, 293–294.
- H. Lei and D. Fan, *Adv. Sci.*, 2022, **9**, 2201425.
- H. Lei and D. Fan, *Chem. Eng. J.*, 2021, **421**, 129578.
- C. Korupalli, H. Li, N. Nguyen, F.-L. Mi, Y. Chang, Y.-J. Lin and H.-W. Sung, *Adv. Healthcare Mater.*, 2021, **10**, 2001384.
- J. Lan, L. Shi, W. Xiao, X. Zhang and S. Wang, *Adv. Mater.*, 2023, **35**, 2301765.
- L. Fan, C. Xiao, P. Guan, Y. Zou, H. Wen, C. Liu, Y. Luo, G. Tan, Q. Wang, Y. Li, P. Yu, L. Zhou and C. Ning, *Adv. Healthcare Mater.*, 2022, **11**, 2101556.
- M. Verdes, K. Mace, L. Margetts and S. Cartmell, *Curr. Opin. Biotechnol.*, 2022, **75**, 102710.
- B. Liu, R. Fu, Z. Duan, C. Zhu, J. Deng and D. Fan, *Composites, Part B*, 2022, **236**, 109804.
- X. Wang, W. Zhang, Q. Zhou and F. Ran, *Chem. Eng. J.*, 2023, **452**, 139491.
- C. Yu, F. Yao and J. Li, *Acta Biomater.*, 2022, **139**, 4–21.
- P. A. Korevaar, C. N. Kaplan, A. Grinthal, R. M. Rust and J. Aizenberg, *Nat. Commun.*, 2020, **11**, 386.
- C. Gao, S. Song, Y. Lv, J. Huang and Z. Zhang, *Macromol. Biosci.*, 2022, **22**, 2200051.
- H. Li, J. Cao, R. Wan, V. R. Feig, C. M. Tringides, J. Xu, H. Yuk and B. Lu, *Adv. Mater.*, 2025, **37**, 2415151.
- B. Lu, H. Yuk, S. Lin, N. Jian, K. Qu, J. Xu and X. Zhao, *Nat. Commun.*, 2019, **10**, 1043.
- J. Liu, J. Garcia, L. M. Leahy, R. Song, D. Mullarkey, B. Fei, A. Dervan, I. V. Shvets, P. Stamenov, W. Wang, F. J. O'Brien, J. N. Coleman and V. Nicolosi, *Adv. Funct. Mater.*, 2023, **33**, 2214196.
- H. Wang, T. Zhuang, J. Wang, X. Sun, Y. Wang, K. Li, X. Dai, Q. Guo, X. Li, D. Chong, B. Chen and J. Yan, *Adv. Mater.*, 2023, **35**, 2302919.
- C. Yu, Z. Yue, H. Zhang, M. Shi, M. Yao, Q. Yu, M. Liu, B. Guo, H. Zhang, L. Tian, H. Sun, F. Yao and J. Li, *Adv. Funct. Mater.*, 2023, **33**, 2211023.
- Y. Wan, N. Qin, Y. Wang, Q. Zhao, Q. Wang, P. Yuan, Q. Wen, H. Wei, X. Zhang and N. Ma, *Chem. Eng. J.*, 2020, **383**, 123103.
- J. Qin, J. Gao, X. Shi, J. Chang, Y. Dong, S. Zheng, X. Wang, L. Feng and Z.-S. Wu, *Adv. Funct. Mater.*, 2020, **30**, 1909756.
- S. Káčarová, M. Muchová, H. Doudová, L. Münster, B. Hanulíková, K. Valášková, V. Kašpárková, I. Kuřitka, P. Humpolíček, Z. Vichová, O. Vašíček and J. Vicha, *Carbohydr. Polym.*, 2024, **327**, 121640.
- B. Yang, C. Liang, D. Chen, F. Cheng, Y. Zhang, S. Wang, J. Shu, X. Huang, J. Wang, K. Xia, L. Ying, K. Shi, C. Wang, X. Wang, F. Li, Q. Zhao and Q. Chen, *Bioact. Mater.*, 2022, **15**, 103–119.
- A. Serafin, M. Culebras, J. M. Oliveira, J. Koffler and M. N. Collins, *Adv. Compos. Hybrid Mater.*, 2023, **6**, 109.

- 42 X. Kang, X. Li, C. Liu, M. Cai, P. Guan, Y. Luo, Y. Guan, Y. Tian, K. Ren, C. Ning, L. Fan, G. Tan and L. Zhou, *J. Mater. Sci. Technol.*, 2023, **142**, 134–143.
- 43 M. Alipuly, D. Kanzhigitova, A. Bexeitova, P. Askar, D. Kanayeva, S. Adilov and N. Nuraje, *Adv. Compos. Hybrid Mater.*, 2024, **8**, 56.
- 44 C. Zhao, S. Zhou, J. Ma, C. Liu, J. Zhu, S. Ye, Z. Xin, J. Cai, P. Feng and X. Tao, *J. Mater. Chem. A*, 2025, **13**, 5238–5251.
- 45 Z. Yi, F. Zhan, Y. Chen, R. Zhang, H. Lin and L. Zhao, *Chem. Eng. J.*, 2023, **478**, 147261.
- 46 D. Liu, H. Zhou, Y. Zhao, C. Huyan, Z. Wang, H. Torun, Z. Guo, S. Dai, B. B. Xu and F. Chen, *Small*, 2022, **18**, 2203258.
- 47 Y. Wang, H.-Q. Lv, X. Chao, W.-X. Xu, Y. Liu, G.-X. Ling and P. Zhang, *Mil. Med. Res.*, 2022, **9**, 16.
- 48 C. Wang, X. Jiang, H.-J. Kim, S. Zhang, X. Zhou, Y. Chen, H. Ling, Y. Xue, Z. Chen, M. Qu, L. Ren, J. Zhu, A. Libanori, Y. Zhu, H. Kang, S. Ahadian, M. R. Dokmeci, P. Servati, X. He, Z. Gu, W. Sun and A. Khademhosseini, *Biomaterials*, 2022, **285**, 121479.
- 49 Y. Xue, J. Li, T. Jiang, Q. Han, Y. Jing, S. Bai and X. Yan, *Adv. Healthcare Mater.*, 2024, **13**, 2302180.
- 50 J. Jeong, T. H. Kim, S. Park, J. Lee, U. Chae, J.-Y. Jeong, S. Park, S. Kim, I.-J. Cho, Y. Jung and H. Yi, *Chem. Eng. J.*, 2023, **465**, 142966.
- 51 J. Xu, C.-H. Tai, T.-Y. Chen and S.-H. Hsu, *Chem. Eng. J.*, 2022, **446**, 137180.
- 52 H. Esmacili, A. Patino-Guerrero, R. A. Nelson, Jr., N. Karamanova, T. M. Fisher, W. Zhu, F. Perreault, R. Q. Migrino and M. Nikkhah, *ACS Biomater. Sci. Eng.*, 2024, **10**, 2351–2366.
- 53 X.-P. Li, K.-Y. Qu, F. Zhang, H.-N. Jiang, N. Zhang, N. Cheraga, C.-M. Liu, K.-H. Wu, X.-W. Wang and N.-P. Huang, *J. Mater. Chem. B*, 2020, **8**, 8085.
- 54 B. Peña, M. Maldonado, A. J. Bonham, B. A. Aguado, A. Dominguez-Alfaro, M. Laughter, T. J. Rowland, J. Bardill, N. L. Farnsworth, N. Alegret Ramon, M. R. G. Taylor, K. S. Anseth, M. Prato, R. Shandas, T. A. McKinsey, D. Park and L. Mestroni, *ACS Appl. Mater. Interfaces*, 2019, **11**, 18671–18680.
- 55 J. Chen, X. Han, J. Deng, J. Zhang, L. Li, J. Ni, Y. Huang, X. Xie, S. Chen, L. Ke, X. Gao, W. Wang and G. Fan, *Chem. Eng. J.*, 2021, **413**, 127423.
- 56 T. Carvalho, R. Bartolo, S. N. Pedro, B. F. A. Valente, R. J. B. Pinto, C. Vilela, M.-A. Shahbazi, H. A. Santos and C. S. R. Freire, *ACS Appl. Mater. Interfaces*, 2023, **15**, 25860–25872.
- 57 Y. Zhao, Z. Li, S. Song, K. Yang, H. Liu, Z. Yang, J. Wang, B. Yang and Q. Lin, *Adv. Funct. Mater.*, 2019, **29**, 1901474.
- 58 Z. Jia, X. Lv, Y. Hou, K. Wang, F. Ren, D. Xu, Q. Wang, K. Fan, C. Xie and X. Lu, *Bioact. Mater.*, 2021, **6**, 2676–2687.
- 59 H. Cui, W. Jiang, C. Wang, X. Ji, Y. Liu, G. Yang, J. Chen, G. Lyu and Y. Ni, *Composites, Part B*, 2021, **225**, 109316.
- 60 J. Yang, Y. Chen, L. Zhao, Z. Feng, K. Peng, A. Wei, Y. Wang, Z. Tong and B. Cheng, *Composites, Part B*, 2020, **197**, 108139.
- 61 X. Song, X. Wang, J. Zhang, S. Shen, W. Yin, G. Ye, L. Wang, H. Hou and X. Qiu, *Biomaterials*, 2021, **273**, 120811.
- 62 M. Jia and M. Rolandi, *Adv. Healthcare Mater.*, 2020, **9**, 1901372.
- 63 Q. Wang, W. Qiu, H. Liu, X. Li, X. Qin, X. Wang, J. Yu, B. Li, F. Li, L. Huang and D. Wu, *Composites, Part B*, 2022, **242**, 110098.
- 64 X. Hu, P. Zhang, J. Liu, H. Guan, R. Xie, L. Cai, J. Guo, L. Wang, Y. Tian and X. Qiu, *Chem. Eng. J.*, 2022, **446**, 136988.
- 65 E. A. Kiyotake, M. D. Martin and M. S. Detamore, *Acta Biomater.*, 2022, **139**, 43–64.
- 66 S. Yang, J. Pan, H. Fu, J. Zheng, F. Chen, M. Zhang, Z. Gong, K. Liang, C. Wang, J. Lai, X. Fang and J. Zhu, *Adv. Compos. Hybrid Mater.*, 2025, **8**, 185.
- 67 R. Yu, H. Zhang and B. Guo, *Nano-Micro Lett.*, 2021, **14**, 1.
- 68 X. Lin, M. Zhang, W. Lv, J. Li, R. Huang and Y. Wang, *Adv. Funct. Mater.*, 2024, **34**, 2310845.
- 69 S. Yao, Y. Yang, C. Li, K. Yang, X. Song, C. Li, Z. Cao, H. Zhao, X. Yu, X. Wang and L.-N. Wang, *Bioact. Mater.*, 2024, **35**, 534–548.
- 70 L. Ye, H. Ji, J. Liu, C.-H. Tu, M. Kappl, K. Koynov, J. Vogt and H.-J. Butt, *Adv. Mater.*, 2021, **33**, 2102981.
- 71 J. Park, J. Kim, G. Choe, Y. Jung and J. Y. Lee, *Biomaterials*, 2025, **317**, 123103.
- 72 X. Ding, Y. Yu, L. Shang and Y. Zhao, *ACS Nano*, 2022, **16**, 19533–19542.
- 73 J. Park, N. Jeon, S. Lee, G. Choe, E. Lee and J. Y. Lee, *Chem. Eng. J.*, 2022, **446**, 137344.
- 74 Q. Zhou, H. Dai, Y. Yan, Z. Qin, M. Zhou, W. Zhang, G. Zhang, R. Guo and X. Wei, *Adv. Healthcare Mater.*, 2024, **13**, 2303143.
- 75 Y.-Z. Zhang, J. K. El-Demellawi, Q. Jiang, G. Ge, H. Liang, K. Lee, X. Dong and H. N. Alshareef, *Chem. Soc. Rev.*, 2020, **49**, 7229–7251.
- 76 H. Zheng, S. Wang, F. Cheng, X. He, Z. Liu, W. Wang, L. Zhou and Q. Zhang, *Chem. Eng. J.*, 2021, **424**, 130148.
- 77 L. Zhou, H. Zheng, Z. Liu, S. Wang, Z. Liu, F. Chen, H. Zhang, J. Kong, F. Zhou and Q. Zhang, *ACS Nano*, 2021, **15**, 2468–2480.
- 78 Q. Yu, S. Jin, S. Wang, H. Xiao and Y. Zhao, *Chem. Eng. J.*, 2023, **452**, 139252.
- 79 X. Ren, M. Xiao, Y. Xu, Y. Wu, J. Yang, Y. Wang, Y. Hu, Z. Jiang, X. Li, Z. Shen, S. Hu and M. Tang, *Chem. Eng. J.*, 2024, **481**, 148791.
- 80 M. Lee, J. Park, G. Choe, S. Lee, B. G. Kang, J. H. Jun, Y. Shin, M. C. Kim, Y. S. Kim, Y. Ahn and J. Y. Lee, *ACS Nano*, 2023, **17**, 12290–12304.
- 81 M. Li, J. Chen, M. Shi, H. Zhang, P. X. Ma and B. Guo, *Chem. Eng. J.*, 2019, **375**, 121999.
- 82 M. Talikowska, X. Fu and G. Lisak, *Biosens. Bioelectron.*, 2019, **135**, 50–63.
- 83 M. Li, Y. Liang, J. He, H. Zhang and B. Guo, *Chem. Mater.*, 2020, **32**, 9937–9953.
- 84 M. Azizi-Lalabadi, H. Hashemi, J. Feng and S. M. Jafari, *Adv. Colloid Interface Sci.*, 2020, **284**, 102250.

- 85 K. Yan, Y. Qin, J. Xue, J. Wang, G. Wang, N. Wang and Y. Chu, *Chem. Eng. J.*, 2024, **484**, 149363.
- 86 S. He, J. Huang, Q. Zhang, W. Zhao, Z. Xu and W. Zhang, *Adv. Funct. Mater.*, 2021, **31**, 2105198.
- 87 H. Wang, R. Zheng, P. He, X. Li, Z. Shi and G. Yang, *Adv. Compos. Hybrid Mater.*, 2024, **7**, 10.
- 88 M. Maruthapandi, K. Sharma, J. H. T. Luong and A. Gedanken, *Carbohydr. Polym.*, 2020, **243**, 116474.
- 89 M.-Y. Xia, Y. Xie, C.-H. Yu, G.-Y. Chen, Y.-H. Li, T. Zhang and Q. Peng, *J. Controlled Release*, 2019, **307**, 16–31.
- 90 Y. Li, X. Liu, L. Tan, Z. Cui, X. Yang, Y. Zheng, K. W. K. Yeung, P. K. Chu and S. Wu, *Adv. Funct. Mater.*, 2018, **28**, 1800299.
- 91 S. Wang, Y. Qiao, X. Liu, S. Zhu, Y. Zheng, H. Jiang, Y. Zhang, J. Shen, Z. Li, Y. Liang, Z. Cui, P. K. Chu and S. Wu, *Adv. Funct. Mater.*, 2023, **33**, 2210098.
- 92 J. He, M. Shi, Y. Liang and B. Guo, *Chem. Eng. J.*, 2020, **394**, 124888.
- 93 Z. Yang, H. Zheng, H. Yin, L. Zhou, Q. Zhang and B. Zhang, *Chem. Eng. J.*, 2023, **471**, 144634.
- 94 W. Wang, B. Jia, H. Xu, Z. Li, L. Qiao, Y. Zhao, H. Huang, X. Zhao and B. Guo, *Chem. Eng. J.*, 2023, **468**, 143362.
- 95 L. Deng, C. Du, P. Song, T. Chen, S. Rui, D. G. Armstrong and W. Deng, *Oxid. Med. Cell. Longevity*, 2021, **2021**, 8852759.
- 96 Y. Zhang, M. Li, Y. Wang, F. Han, K. Shen, L. Luo, Y. Li, Y. Jia, J. Zhang, W. Cai, K. Wang, M. Zhao, J. Wang, X. Gao, C. Tian, B. Guo and D. Hu, *Bioact. Mater.*, 2023, **26**, 323–336.
- 97 Y. Liang, M. Li, Y. Yang, L. Qiao, H. Xu and B. Guo, *ACS Nano*, 2022, **16**, 3194–3207.
- 98 T. Zhu, Y. Ni, G. M. Biesold, Y. Cheng, M. Ge, H. Li, J. Huang, Z. Lin and Y. Lai, *Chem. Soc. Rev.*, 2023, **52**, 473–509.
- 99 F. Oohashi, K. Ogai, N. Takahashi, D. Arisandi, T. Urai, J. Sugama and M. Oe, *Wound Repair Regen.*, 2022, **30**, 190–197.
- 100 X. Liu, S. Tian, S. Xu, W. Lu, C. Zhong, Y. Long, Y. Ma, K. Yang, L. Zhang and J. Yang, *Biosens. Bioelectron.*, 2022, **214**, 114528.
- 101 W. Li, Y. Yu, R. Huang, X. Wang, P. Lai, K. Chen, L. Shang and Y. Zhao, *Adv. Sci.*, 2023, **10**, 2301479.
- 102 K. Shen, Z. Liu, R. Xie, Y. Zhang, Y. Yang, X. Zhao, Y. Zhang, A. Yang and Y. Cheng, *Mater. Horiz.*, 2023, **10**, 2096–2108.
- 103 F. Chen, M. Wu, Q. Dong, M. Ke, X. Liang, J. Ai, Q. Cheng, L. Cai, Z. Tong and Y. Chen, *Composites, Part B*, 2022, **238**, 109903.
- 104 M. Shan, X. Chen, X. Zhang, S. Zhang, L. Zhang, J. Chen, X. Wang and X. Liu, *Adv. Healthcare Mater.*, 2024, **13**, 2303876.
- 105 C. Xue, Y. Zhao, Y. Liao and H. Zhang, *Adv. Mater.*, 2025, **37**, 2416275.